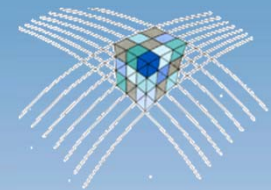


Change detection of urban objects using 3D point clouds (1)

Uwe **STILLA**

TUM - Photogrammetry and Remote Sensing

University of Twente - NCG seminar on point clouds
2020-JUN-11



NCG





Photogrammetry and
Remote Sensing



Change detection using 3d point clouds

- Change detection as subject of PhD work at TUM-PF
 - Mobile thermal mapping of buildings (terrestrial) [Zhu et al., 2019]
 - Airborne thermal mapping of buildings [Hoegner & Stilla, 2018]
 - **Change detection of urban areas by oblique ALS (Helicopter)**
 - Photogr. construction site monitoring using BIM [Tuttas et al., 2017]
 - Change detection of construction sites from point clouds [Huang, 2019]
 - Street canyon mapping by MLS [Gehring et al., 2019][Zhu et al., 2020]
 - Pedestrian tracking in MLS point clouds [Borgmann et al., 2019]
 - Bathymetric change detection of river beds [Boerner et. al, 2019]
 - Change detection by space-borne SAR [Vilamill & Stilla, 2019]
 - Laser-based indoor mapping and IndoorGML [Tessema et al., 2019]
 - Photogrammetric indoor mapping and BIM [Meyer, 2019]
 - Reconstruction and monitoring of urban trees [Hirt, 2019]
 - Rock fall monitoring in alpine regions [Dinkel et al., 2020]

Change detection using 3d point clouds

- ❑ Automatic **change detection** is of general interest of monitoring dynamic processes which show a confusing situation for human observers
- ❑ Independent on sensors (e.g. photogrammetry, laser scanning, RADAR) the 3D geometry of urban structures is often represented by **point clouds**

Challenges

- ❑ Detection of **small** changes on-the-fly in **extended** urban areas showing complex structures
 - **Example I: Comparison of point clouds [Hebel & Stilla]**
- ❑ Change detection of “**objects of interest**” in a **rapidly** changing environment --> **construction sites**
 - **Example II:** Progress monitoring – Comparison of point clouds and building information models (BIM) [Tuttas & Stilla]



M. Hebel

Research project:

Comparison point cloud-to-point cloud Change detection of urban areas by oblique ALS (Helicopter)

- ❑ Hebel M, Stilla U (2012) Simultaneous calibration of ALS systems and alignment of multiview LiDAR scans of urban areas. IEEE Transactions on Geoscience and Remote Sensing, 50(6): 2364-2379
- ❑ Hebel M, Arens M, Stilla U (2013) Change detection in urban areas by object-based analysis and on-the-fly comparison of multi-view ALS data. ISPRS Journal of Photogrammetry and Remote Sensing 86 (2013): 52–64

ALS, experimental setup, direct georeferencing

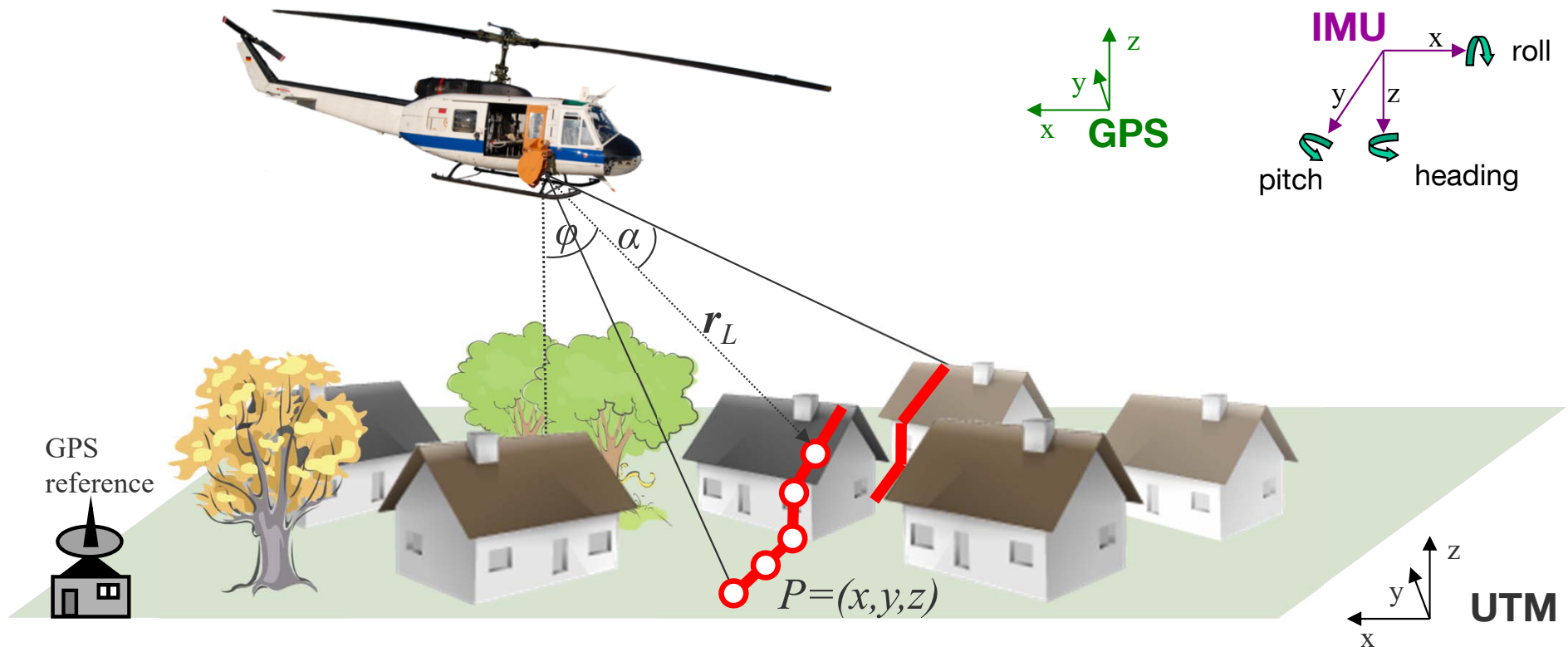
RIEGL LMS-Q560

- full waveform
- polygon mirror
- scan-lines

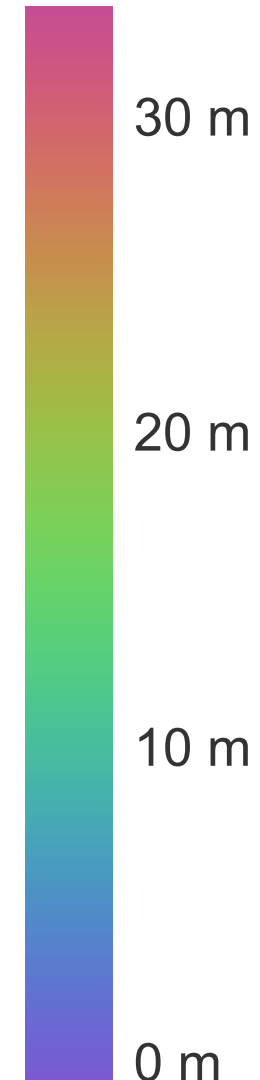
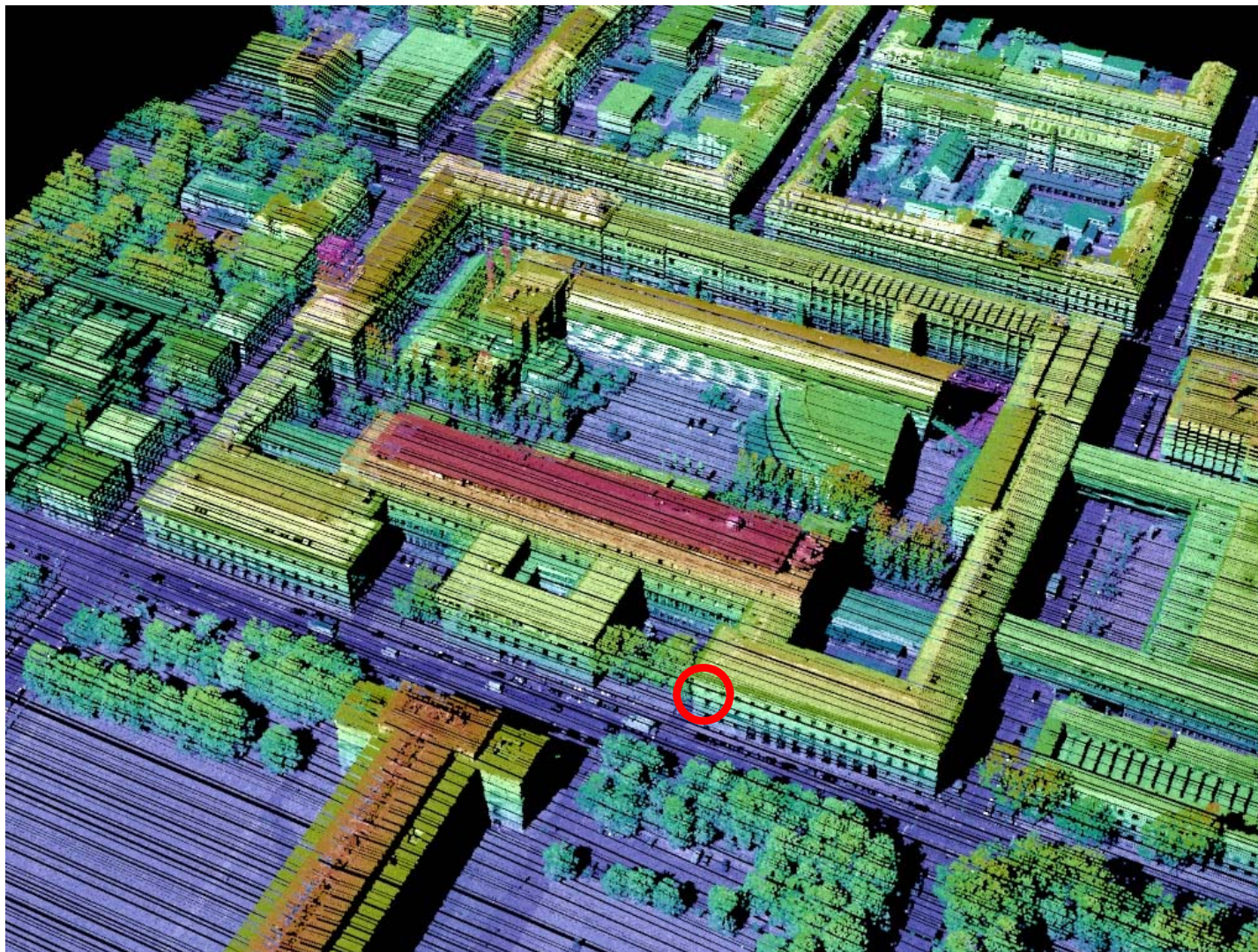


Applanix POS AV 410

- time (UTC)
- position (GPS)
- orientation (IMU)

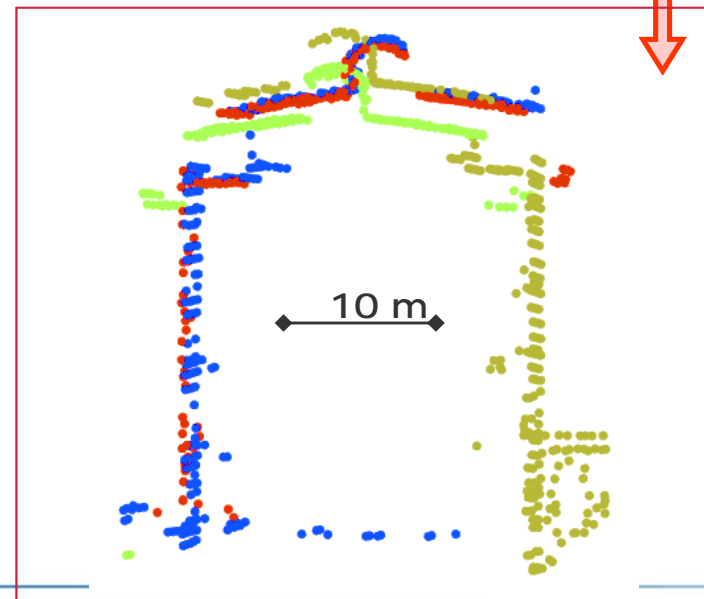
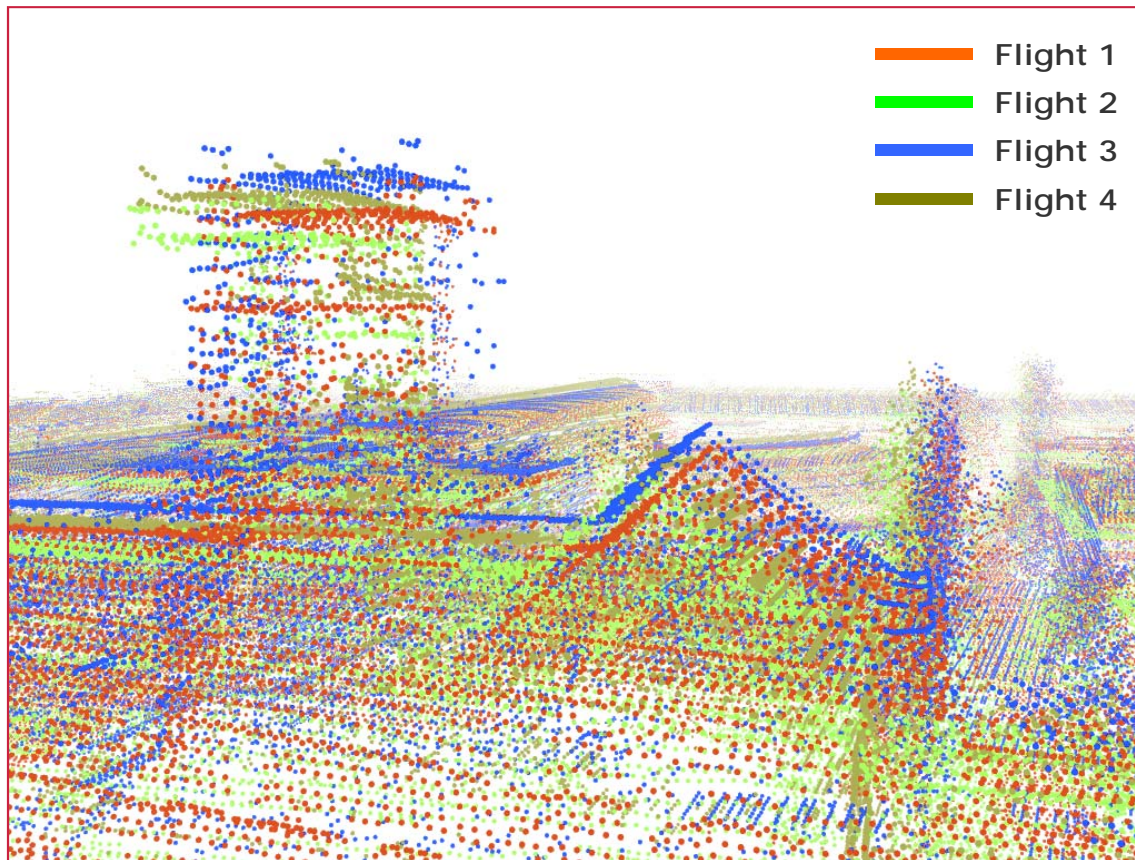


Example: ALS-Flight TUM City Campus 2006



[<https://www.youtube.com/watch?v=FI-EIDL7IIE>]

Elevation above ground



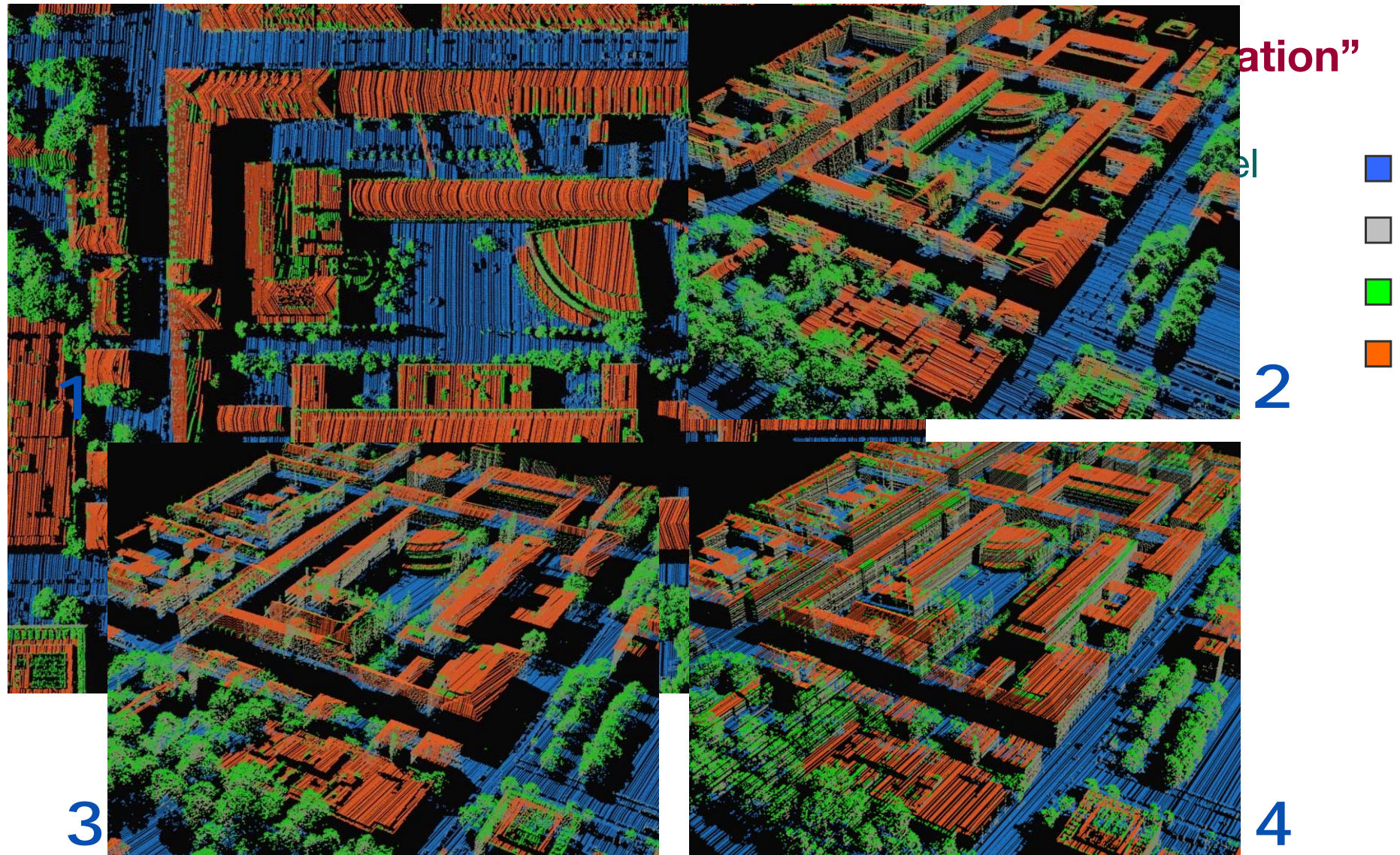
Displacement mainly caused by:

- Inaccurate relative sensor position
- Errors in the navigational data



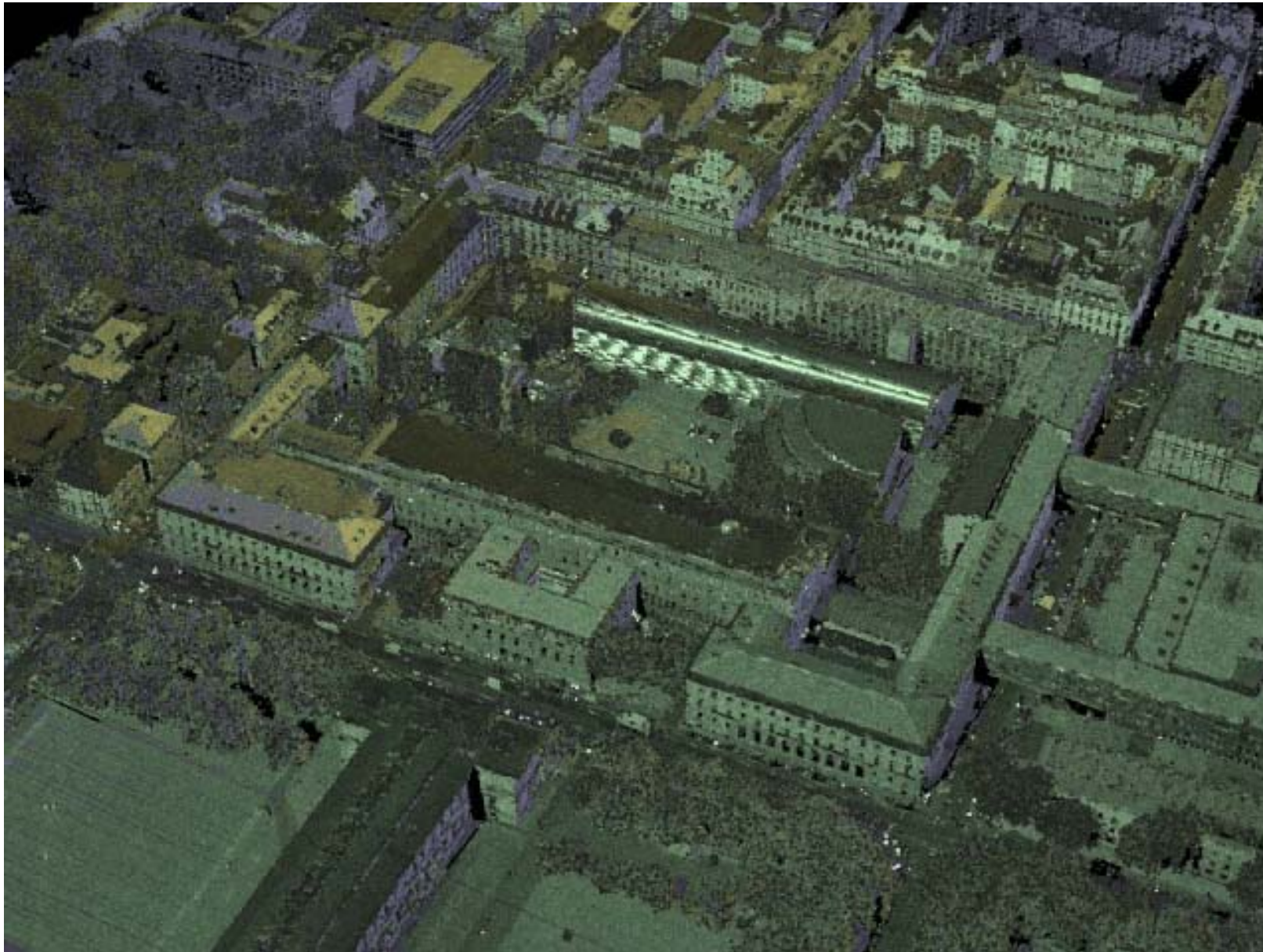
□ “Classification”

- Ground level 
- Facades 
- Vegetation 
- Rooftops 





[<https://www.youtube.com/watch?v=203b-zWlsZ4>]



[<https://www.youtube.com/watch?v=OxV02RqllpY>]

Generation of a database: t_1

- Not time-critical
- Multiple scans of the relevant urban area
- Calibration
- Off-line data processing
- Analysis of the combined (full 3D) point cloud

Database



PPK



Helicopter/UAV mission: t_2

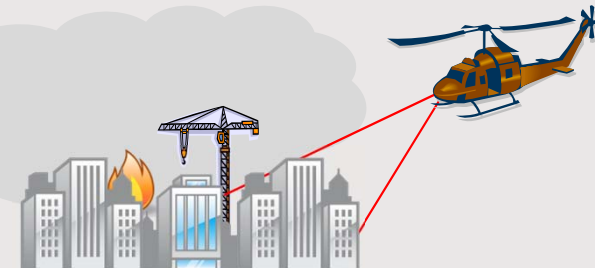
- Oblique forward-looking sensor (obstacle avoidance)
- Degraded GPS accuracy
- Scan-line methods
- Data alignment, terrain referenced navigation

Current ALS data

Comparison,
change detection

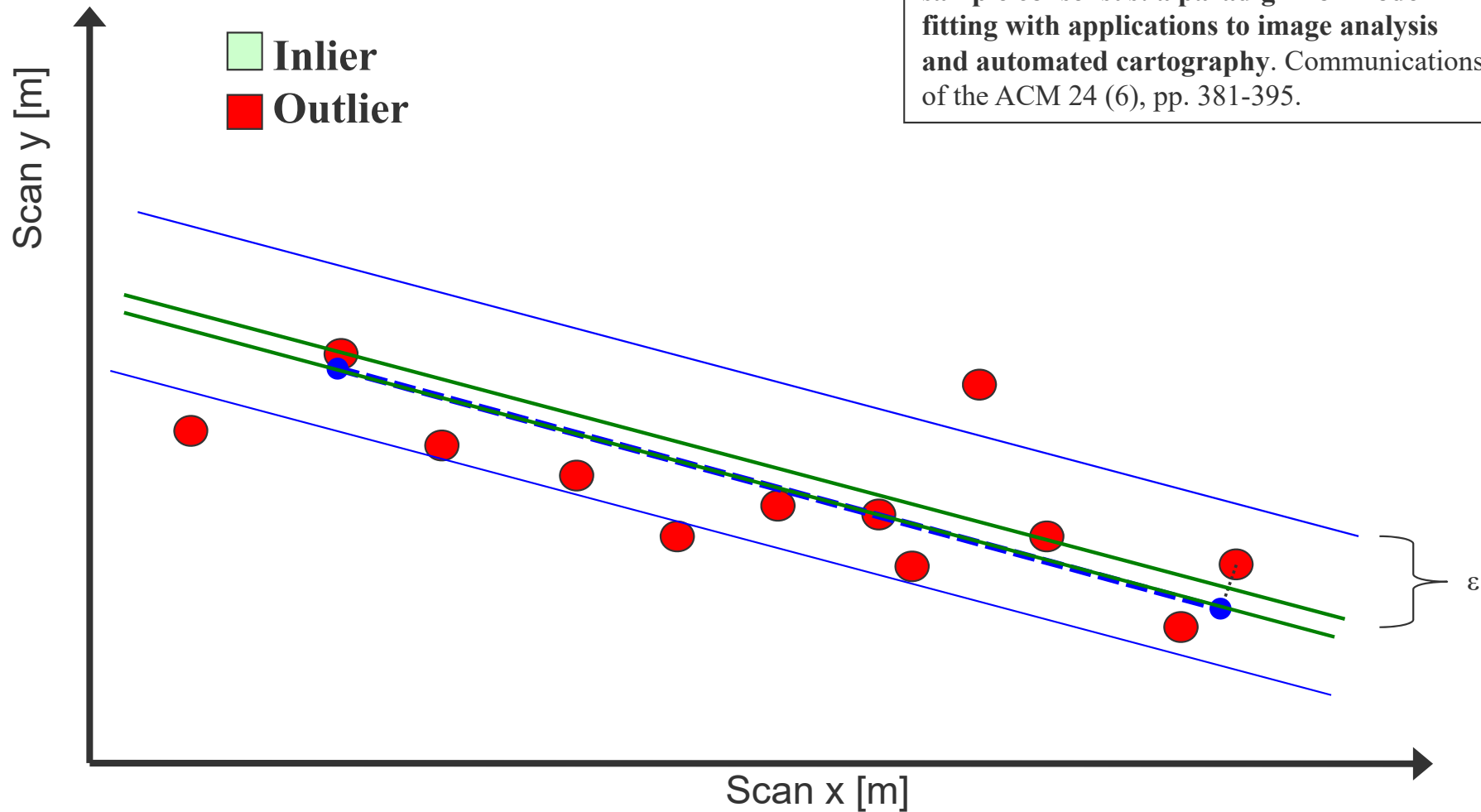


RTK



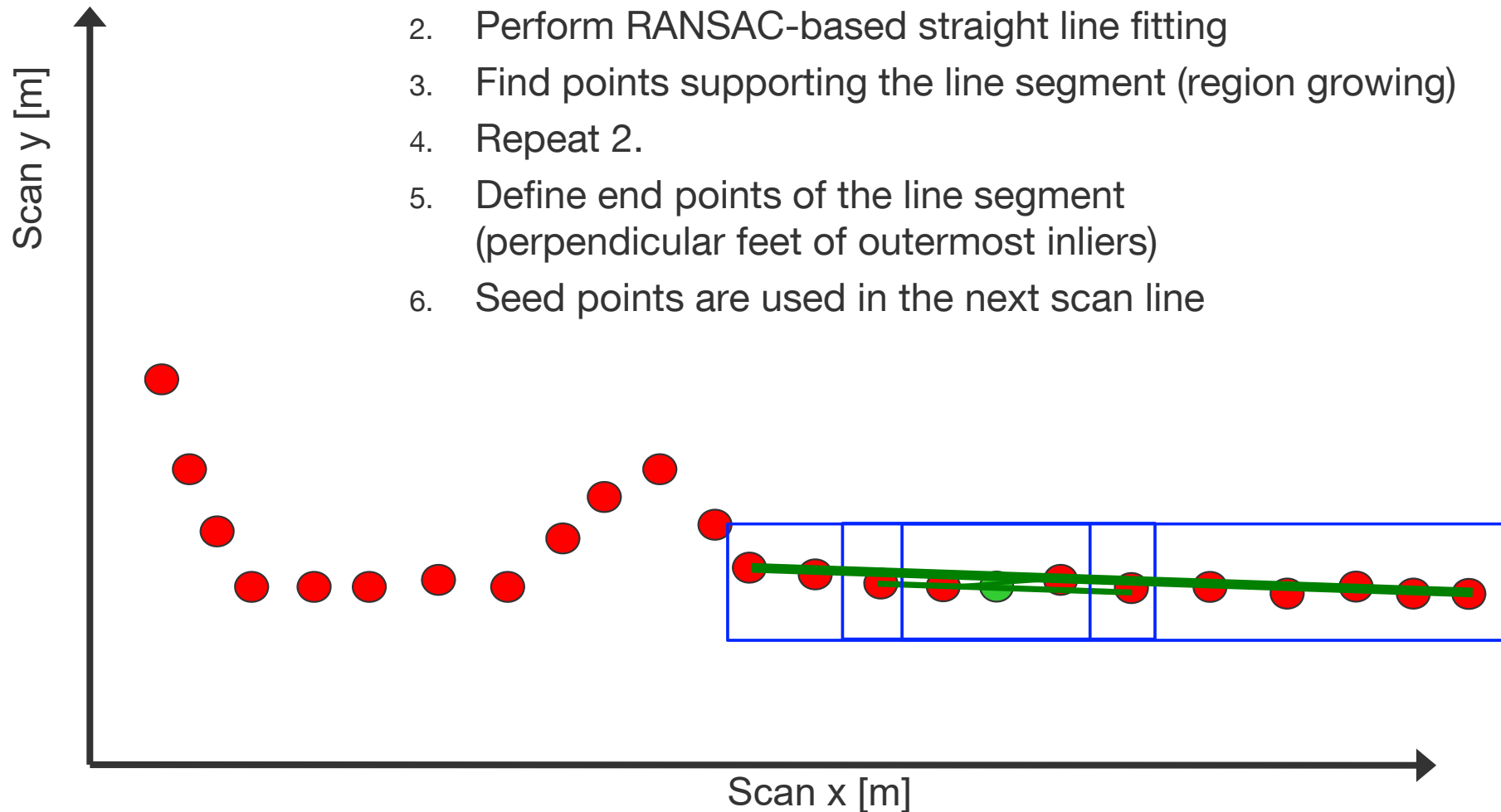
Segmentation of straight line segments

Fischler, M.A., Bolles, R.C., 1981. **Random sample consensus: a paradigm for model fitting with applications to image analysis and automated cartography.** Communications of the ACM 24 (6), pp. 381-395.

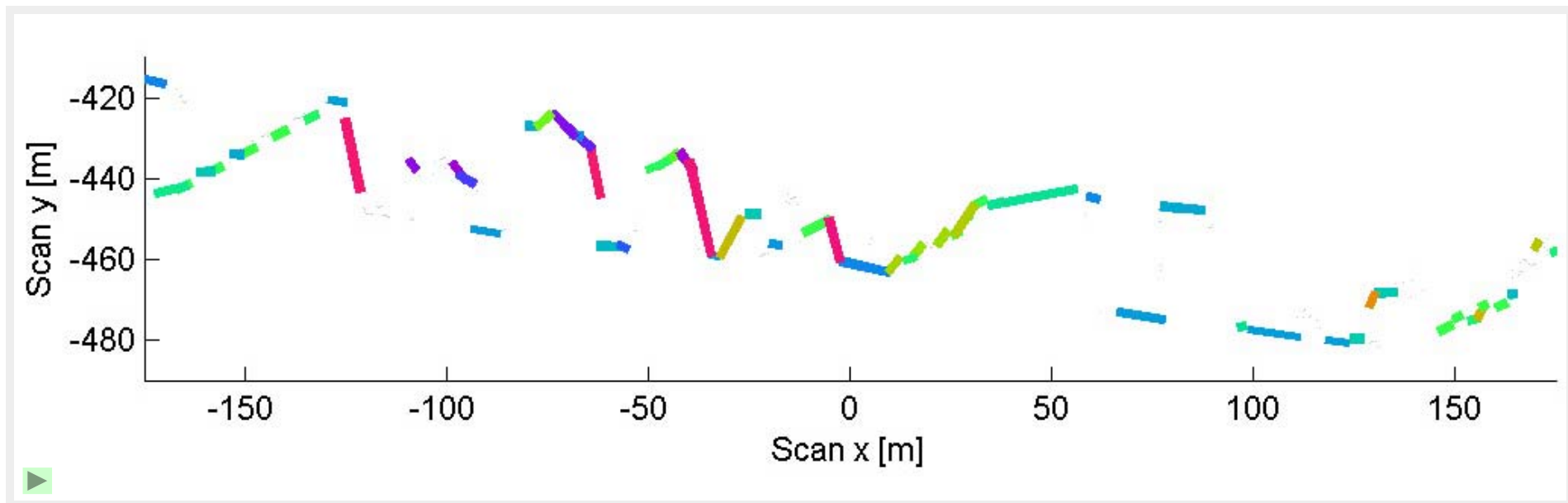


Segmentation of straight line segments

1. Choose position in scan line data
2. Perform RANSAC-based straight line fitting
3. Find points supporting the line segment (region growing)
4. Repeat 2.
5. Define end points of the line segment (perpendicular feet of outermost inliers)
6. Seed points are used in the next scan line

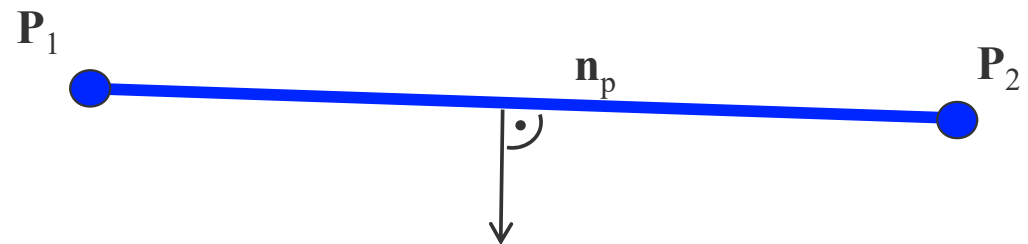


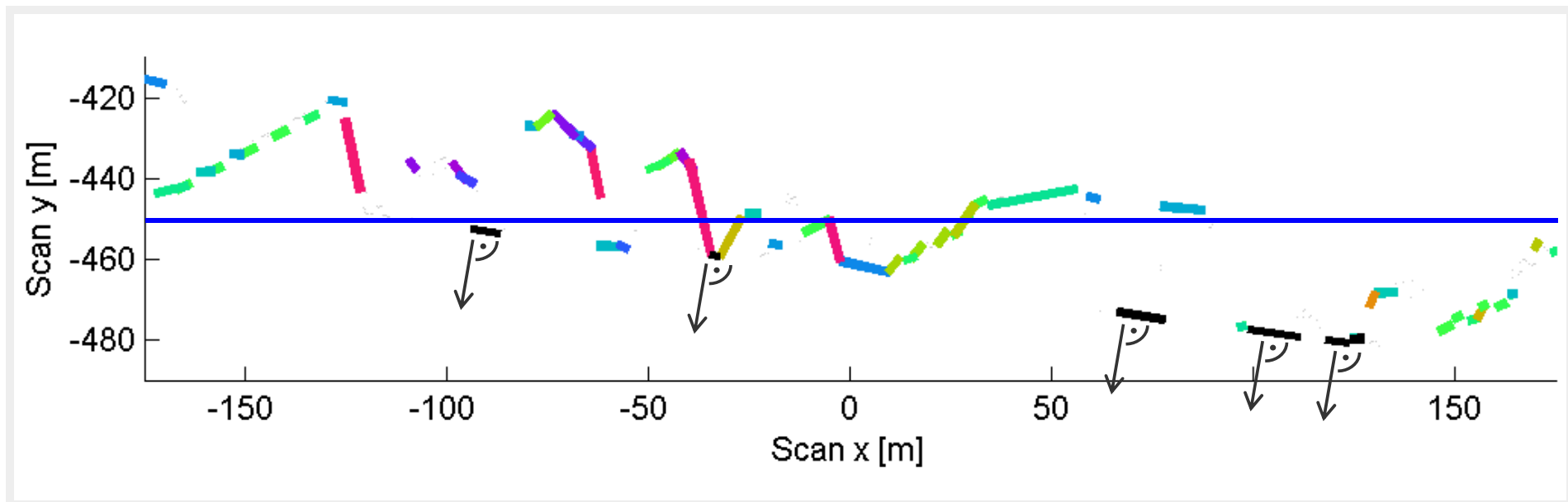
Example: Detected straight line segments



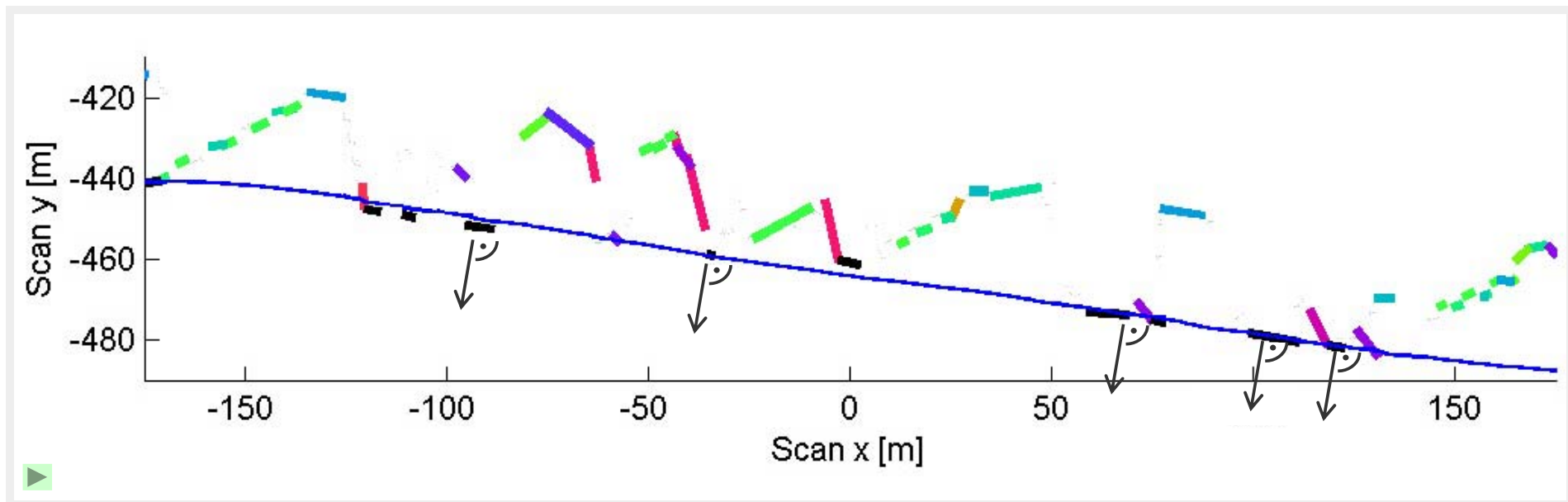
Each line segment:

End points P_1, P_2
 2D normal direction n_p





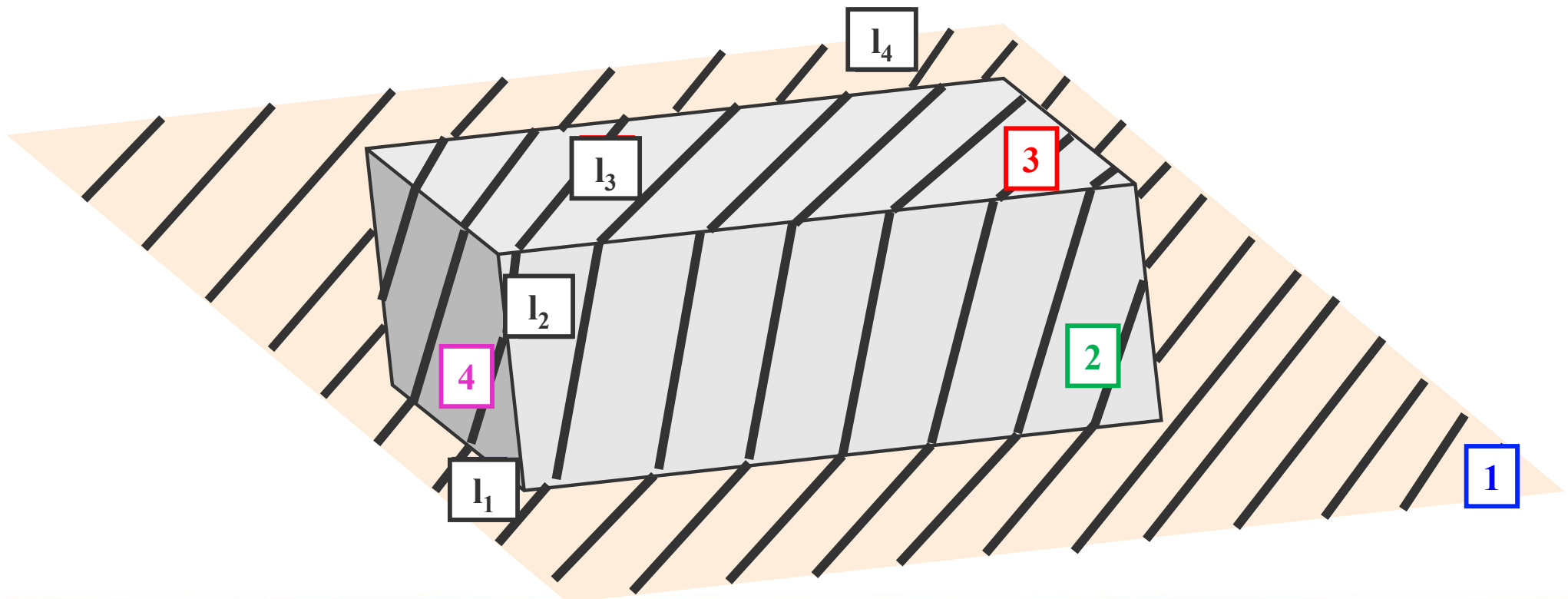
- **Candidates:** No points lying beneath the line segment
- **Ground level** is initialized as average distance to the sensor
- **Candidates contribute** to the estimated ground level
- **Moving average** in time refines ground level
- **Only few initial scan lines** to get a good estimation of the ground level

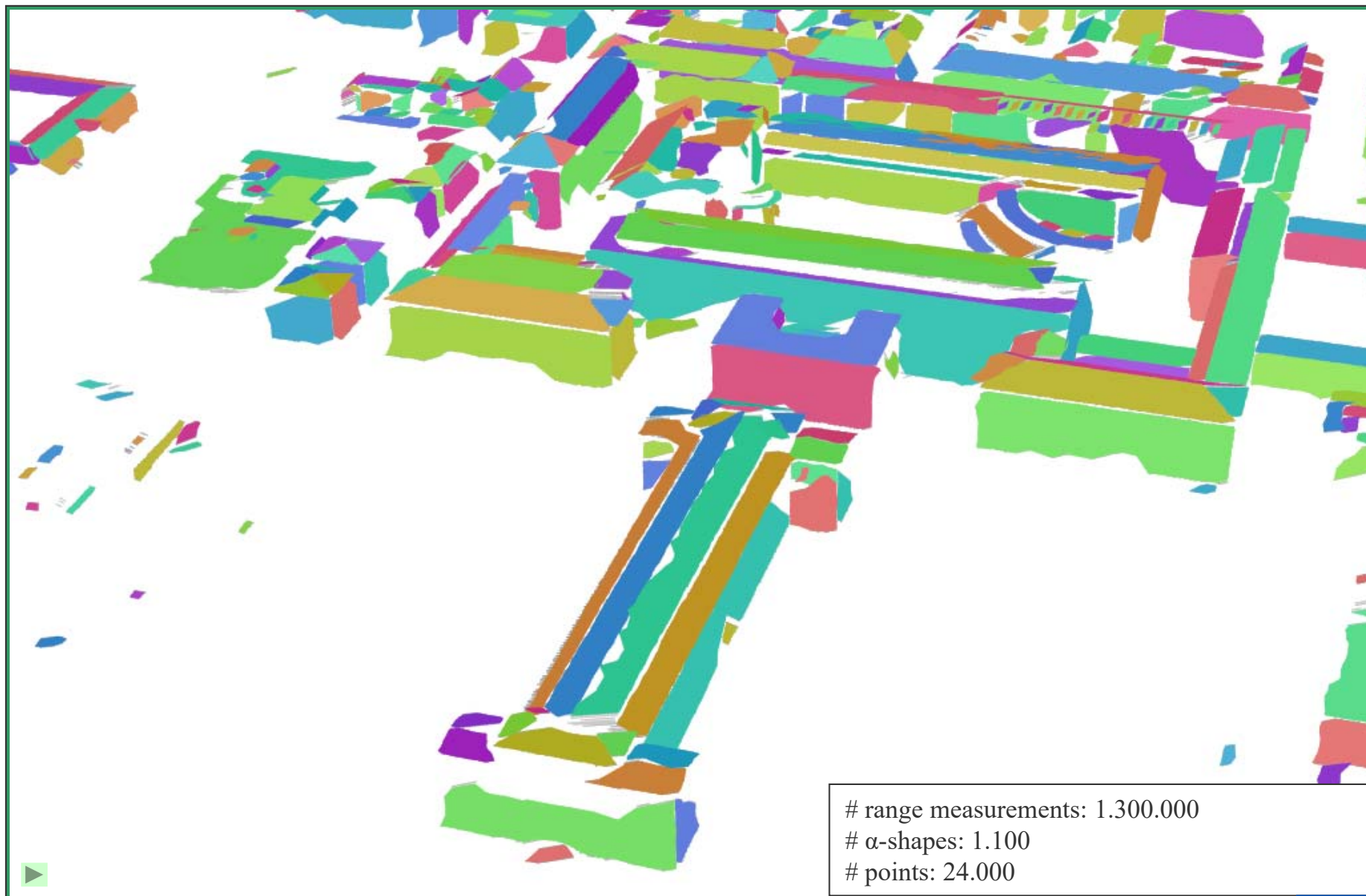


- **Candidates:** No points lying beneath the line segment
- **Ground level** is initialized as average distance to the sensor
- **Candidates contribute** to the estimated ground level
- **Moving average** in time refines ground level
- **Only few initial scan lines** to get a good estimation of the ground level

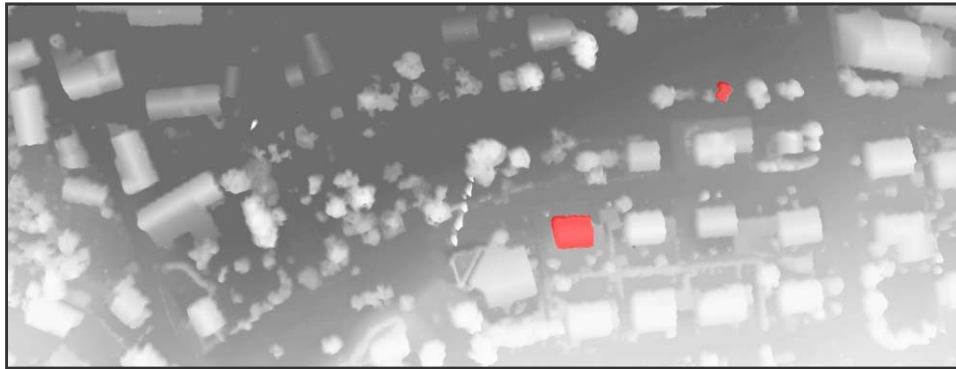
Grouping of line segments over scan lines

- Initialize each new line segment with an increasing unique labeling number
- Check older line segments in the last n (e.g. $n=5$) scan lines for proximity and coplanarity ($d_3 < \epsilon_3$, $d_4 < \epsilon_4$)
- Coplanar line segments are linked (minimum labeling number)
- Repeat until labeling numbers don't change anymore



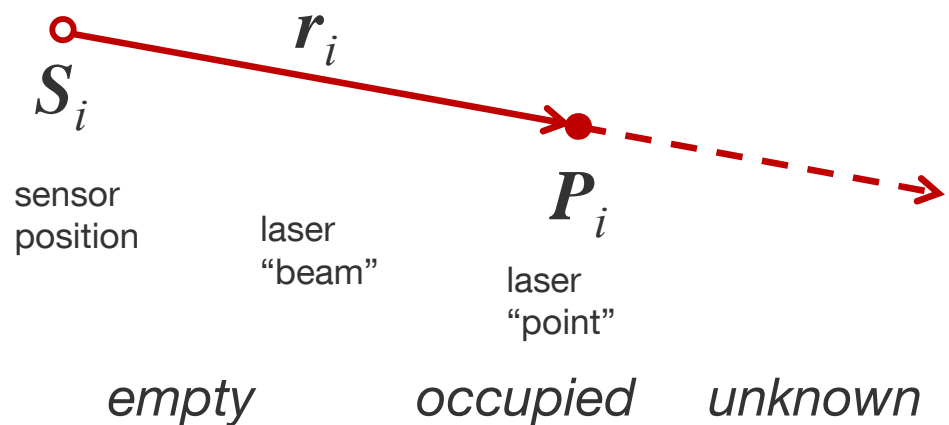


- Common approach: Comparison (difference) of DSMs

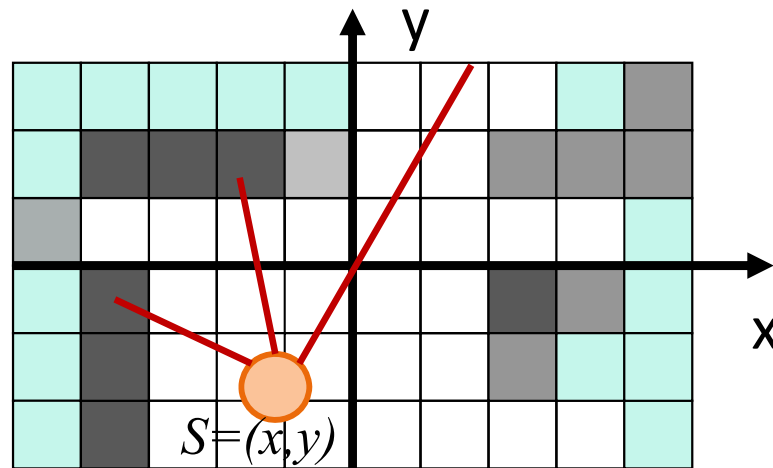


- Interpolation onto 2D grid
- Works best with nadir views (no occlusions)
- e.g., update of maps
- Comparison of point clouds, other information is lost

Our method: Analysis of conflicts between **empty** and **occupied** space



- Occlusions and changes are handled implicitly
- Works well with multi-view data
- Evaluation of single range measurements (real-time capable)

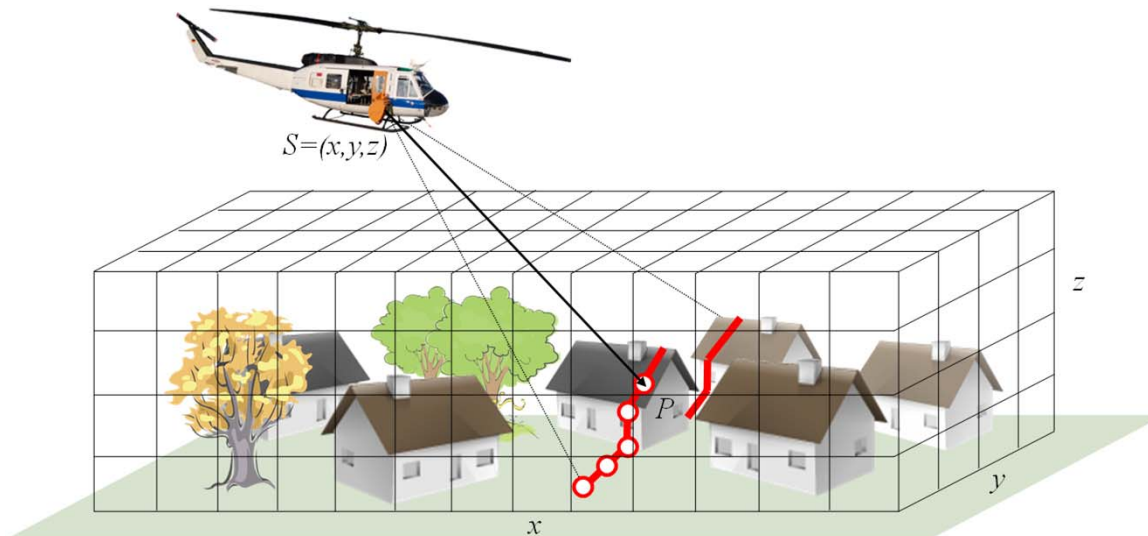


Well known similar approach:

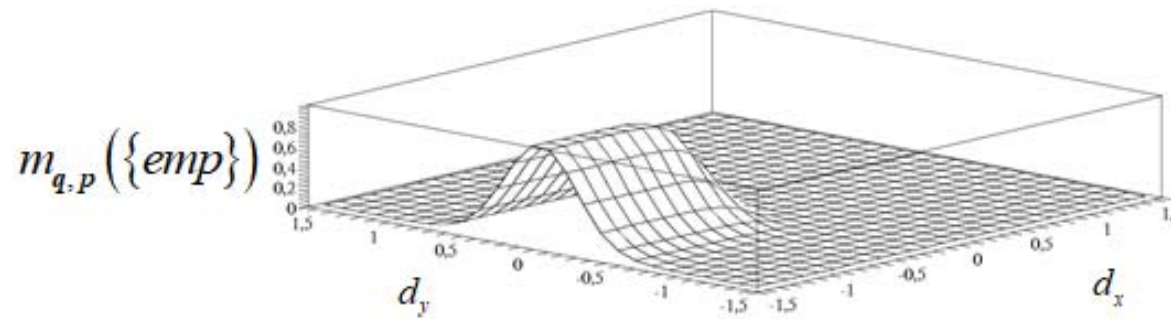
- 2D robot mapping
- Different methods for information fusion:
 - Probabilistic (Bayes)
 - **Dempster-Shafer theory**

Our approach:

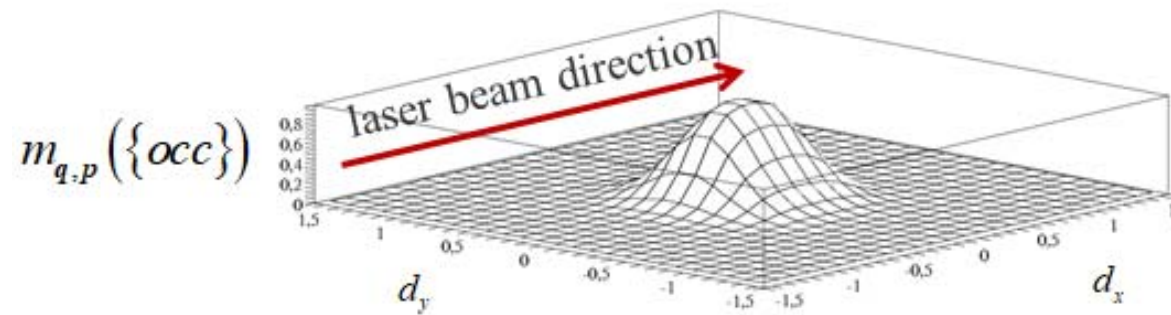
- 3D grid used for search operations
- Cell size comparatively wide
- Occupancy evaluated at the position of the laser points (no interpolation)



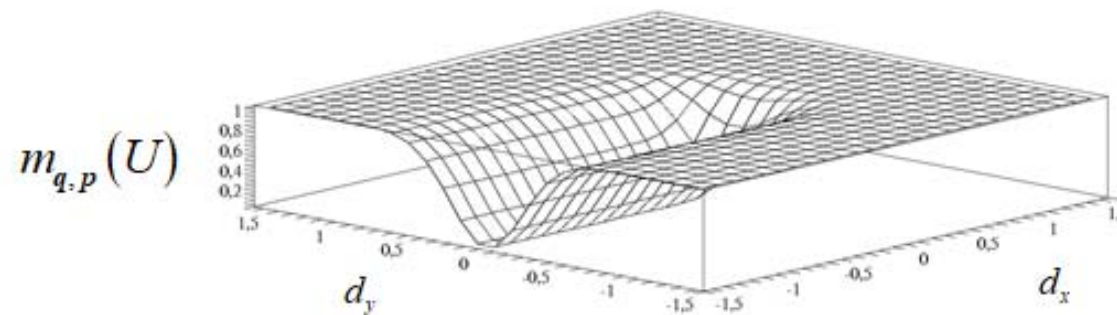
Belief assignment caused by a single laser “beam”



$$\left(1 - \frac{1}{1 + e^{-\lambda d_x - c}}\right) \cdot e^{-\kappa d_y^2}$$



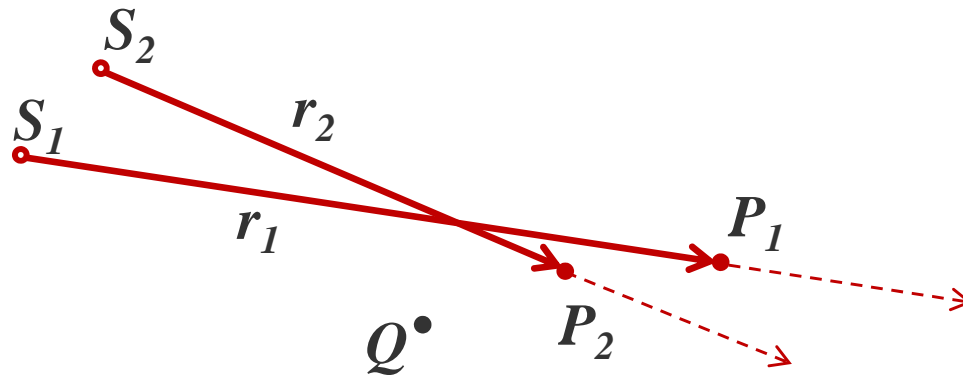
$$\left(\frac{1}{1 + e^{-\lambda d_x - c}} - \frac{1}{1 + e^{-\lambda d_x + c}}\right) \cdot e^{-\kappa d_y^2}$$



$$1 - m_{q,p}(\{emp\}) - m_{q,p}(\{occ\})$$

“degree of ignorance”

Parameters (λ, c, κ) : laser footprint, point positioning accuracy



m_1 : belief assignment at Q
caused by P_1

m_2 : belief assignment at Q
caused by P_2

- Belief masses at a position q caused by laser measurements p_1 and p_2
- Conflicting evidence: $C = m_1(emp)m_2(occ) + m_1(occ)m_2(emp)$
- **Dempster's rule of combination**

$$m(e) = \frac{m_1(e)m_2(e) + m_1(e)m_2(U) + m_1(U)m_2(e)}{1 - C}$$

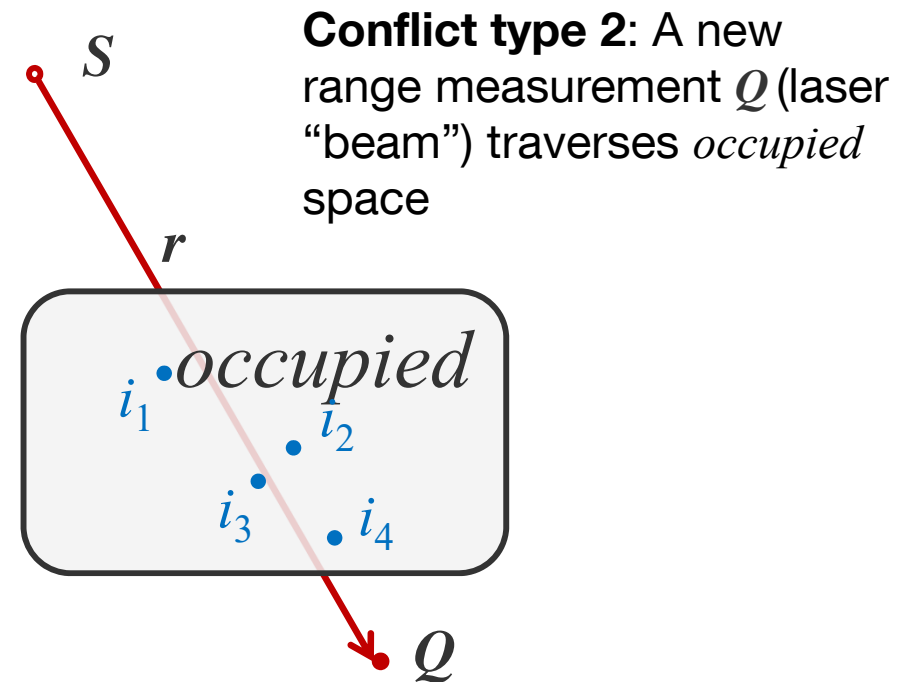
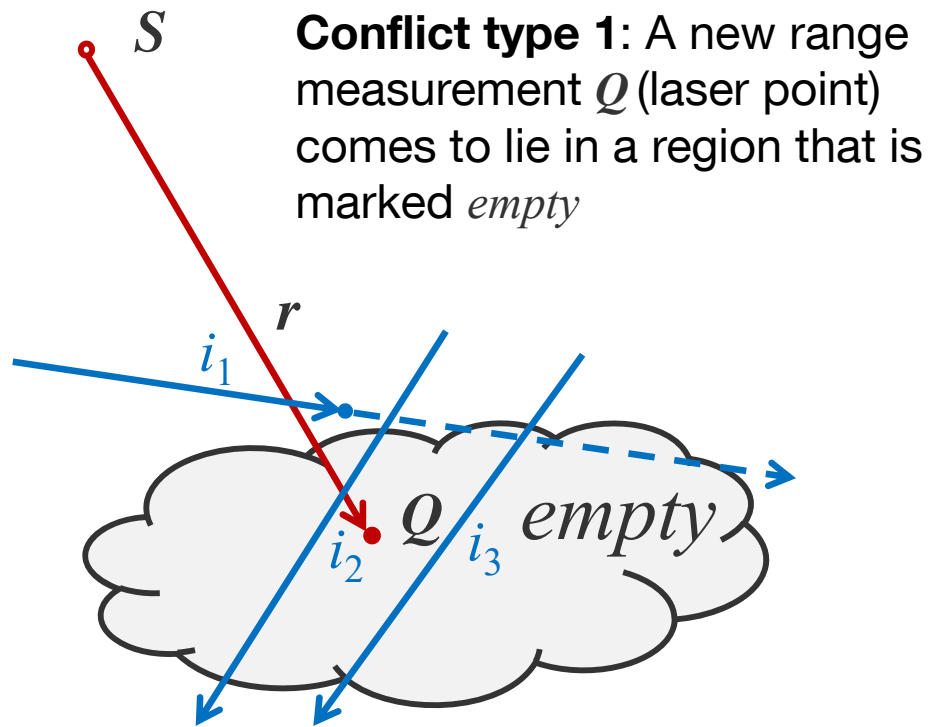
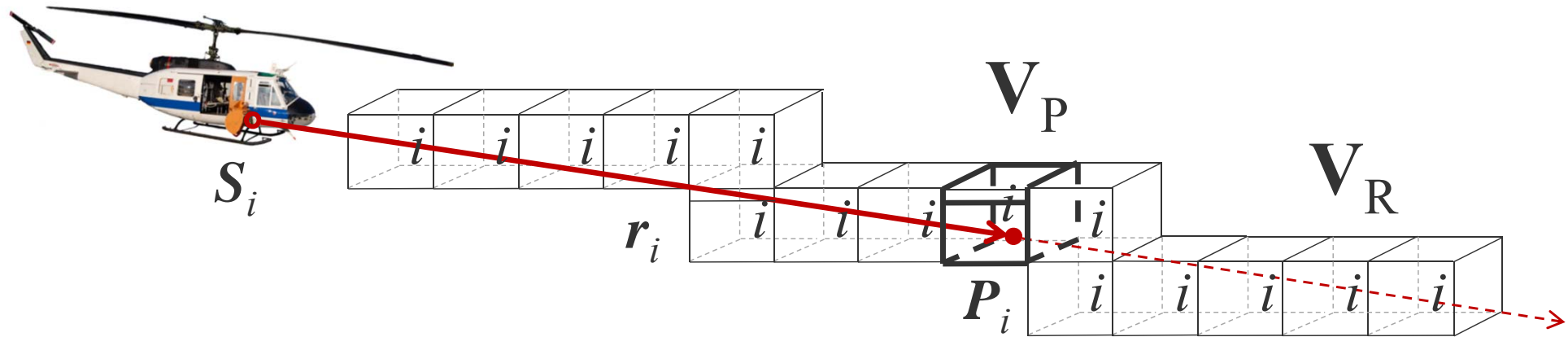
$$m(o) = \frac{m_1(o)m_2(o) + m_1(o)m_2(U) + m_1(U)m_2(o)}{1 - C}$$

$$m(U) = \frac{m_1(U) \cdot m_2(U)}{1 - C} \quad m(\emptyset) = 0$$

$$m = m_1 \oplus m_2$$

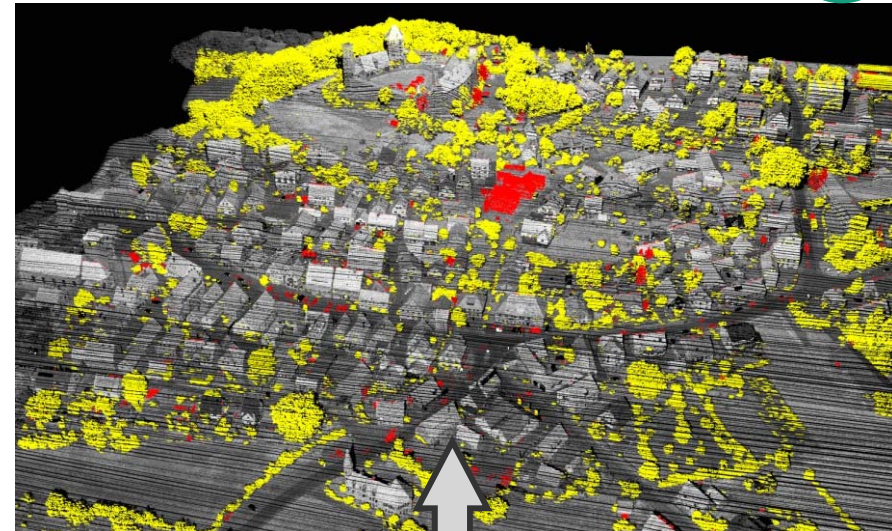
\oplus is commutative and associative

Idea: Changes correspond to conflicting evidence





t_1



t_2

■ type 2 conflict

■ type 1 conflict

Abenberg 04/18/2008:

- combination of 4 views / aspects (45° oblique view)
- 5,400,000 points
- 500 x 600 x 90 m
- V_R, V_P cell size 2 x 2 x 2 m³

Abenberg 08/31/2009:

- one strip (south-to-north)
- 1,500,000 points
- type 1 conflicts can be ascribed to seasonal changes (April / August)

[<https://www.youtube.com/watch?v=GA2UFRDVyD8>]



Testdata find here: [<https://www.pf.bgu.tum.de/en/pub/tst.html>]

2008



2009

The detection principle allows an assessment during the flight

[<https://www.youtube.com/watch?v=t6npBcHvI3o>]

Testdata find here: [<https://www.pf.bgu.tum.de/en/pub/tst.html>]

2009



The detection principle allows an assessment during the flight

[<https://www.youtube.com/watch?v=t6npBcHvl3o>]

Direct comparison

-  Typ 1 Conflict
-  Typ 2 Conflict
-  confirmed planar area
-  unchanched ground
-  unchanged surface



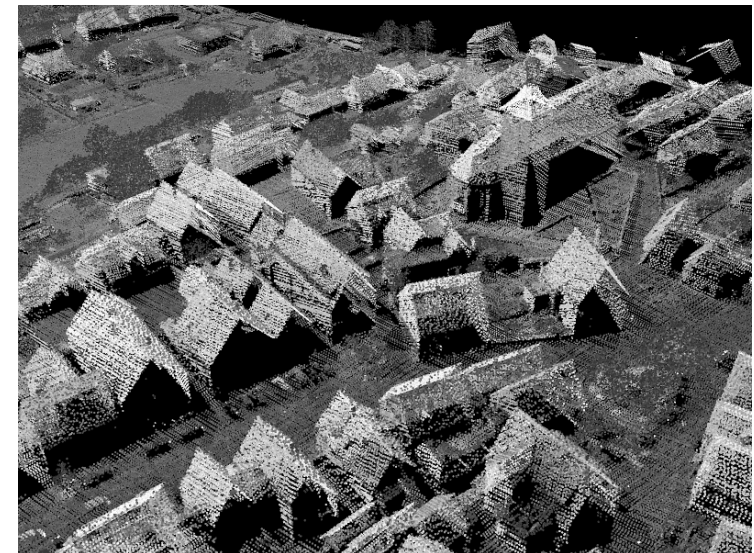
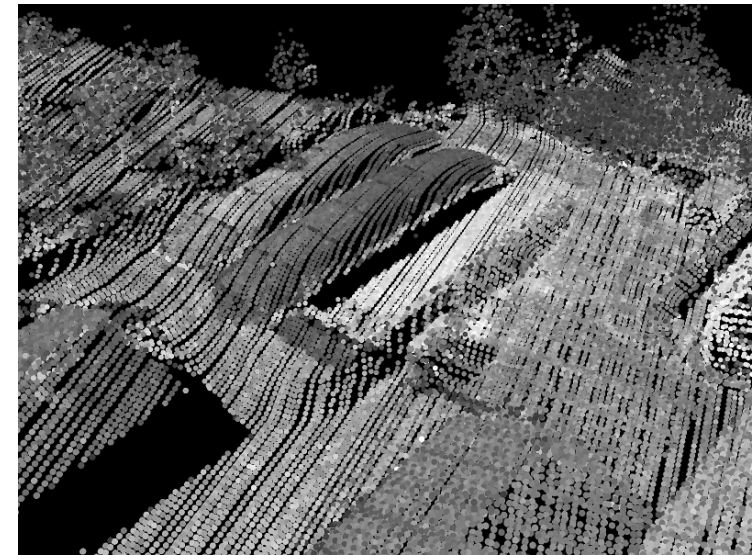
The detection principle allows an assessment during the flight

2009

[<https://www.youtube.com/watch?v=t6npBcHvI3o>]

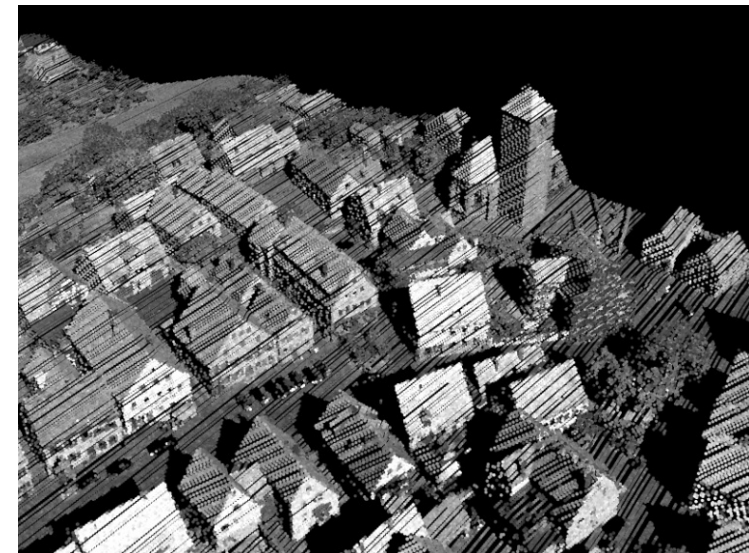
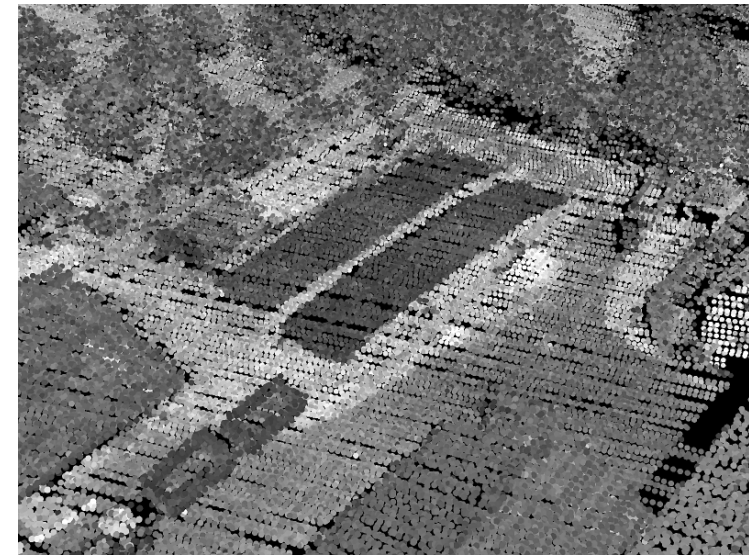
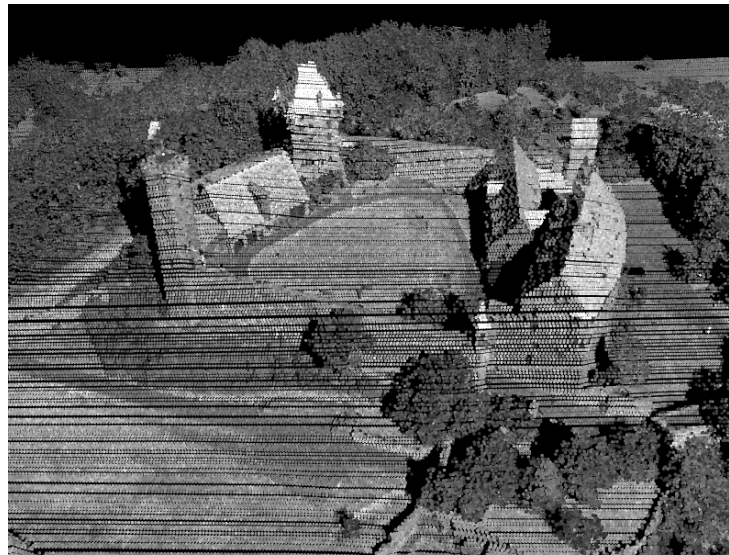
2008

-  Typ 1 Conflict
-  Typ 2 Conflict
-  confirmed planar area
-  unchanched ground
-  unchanged surface
-  unveränderte Vegetation



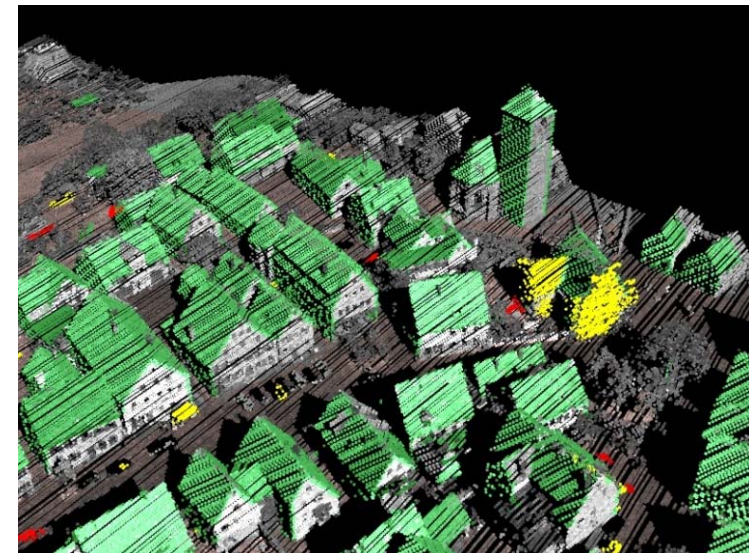
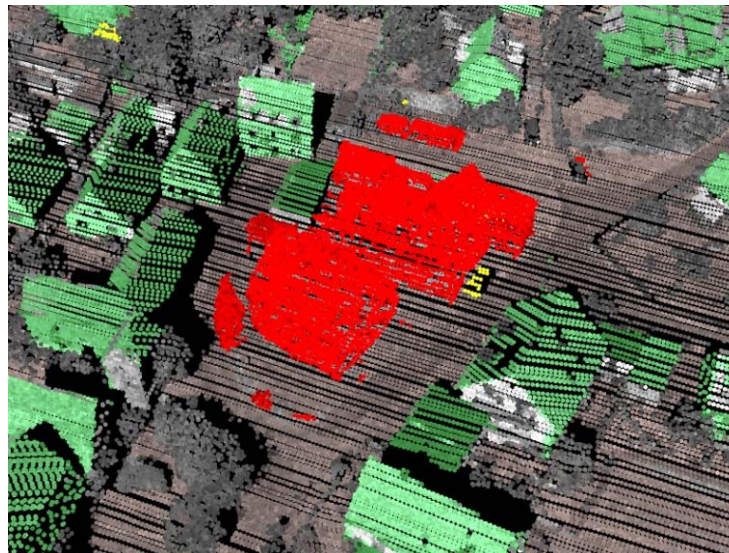
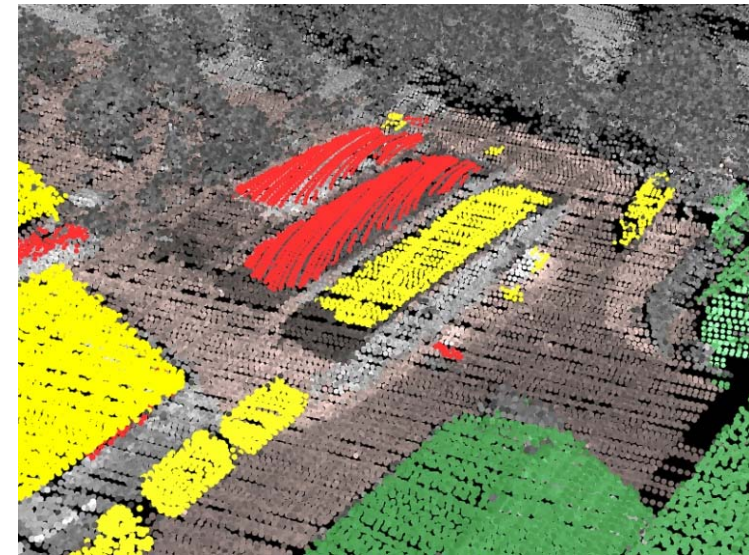
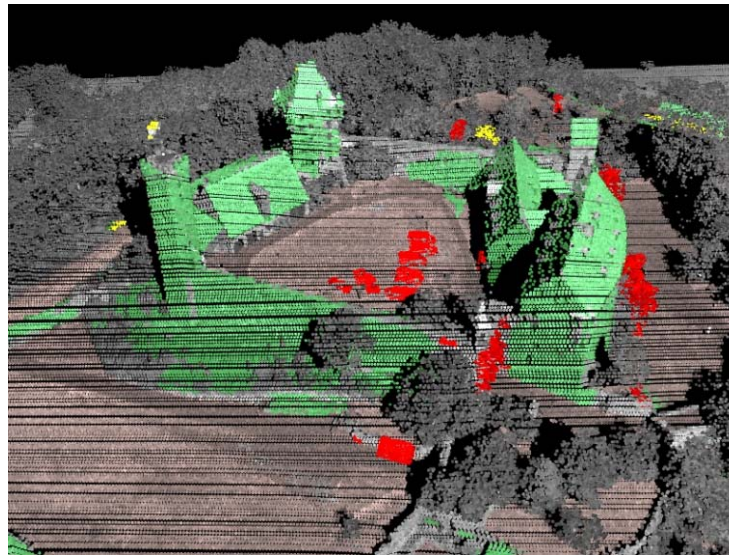
2009

-  Typ 1 Conflict
-  Typ 2 Conflict
-  confirmed planar area
-  unchanched ground
-  unchanged surface
-  unveränderte Vegetation



Changes

-  Typ 1 Conflict
-  Typ 2 Conflict
-  confirmed planar area
-  unchanched ground
-  unchanged surface
-  unveränderte Vegetation



- **Open Access:** Test data set **TUM-MLS-2016**
[<https://www.pf.lrg.tum.de/en/pub/tst.html>]



[https://www.pf.lrg.tum.de/img/div/tum_pf_tst_mls_scn1.gif]

Longer version on YouTube:

[<https://www.youtube.com/watch?v=JMM54vOqwbY>]



[https://www.pf.lrg.tum.de/img/div/tum_pf_tst_mls_lab1.gif]

Longer version on YouTube:

[<https://www.youtube.com/watch?v=vUvrfQYeCZg>]

Description of the test dataset **TUM-MLS-2016** :

- Zhu J, Gehring J, Huang R, Borgmann B, Sun Z, Hoegner L, Hebel M, Xu Y, Stilla U (2020) TUM-MLS-2016: An annotated mobile LiDAR dataset of the TUM city campus for semantic point-cloud interpretation in urban areas. Remote Sensing, 12(11): 1875 [<https://doi.org/10.3390/rs12111875>]

Reference list with links to papers → [<https://www.pf.lrg.tum.de/sta/stilla/pub.html>]

- ❑ Boerner R, Hoegner L, Stilla U (2019) Semantic change detection of river ground points in airborne LiDAR bathymetry data using voxel occupancies. ISPRS Annals of the Photogrammetry, Remote Sensing and Spatial Information Sciences, IV-2/W7: 9–15
- ❑ Borgmann B, Hebel M, Arens M, and Stilla U (2019) Using neural networks to detect objects in MLS point clouds based on local point neighborhoods. ISPRS Annals of the Photogrammetry, Remote Sensing and Spatial Information Sciences, IV-2/W7: 17–24
- ❑ Braun A, Tuttas S, Borrmann A, Stilla U (2020) Improving progress monitoring by fusing point clouds, semantic data and computer vision. Automation in Construction, 116: 103210
- ❑ Dinkel A, Hoegner L, Emmert A, Raffl L, Stilla U (2020) Change detection in photogrammetric point clouds for monitoring of alpine, gravitational mass movement. (in press: ISPRS Annals)
- ❑ Gehring J, Hebel M, Arens M, Stilla U (2019) A fast voxel-based indicator for change detection using low resolution octrees. ISPRS Annals of the Photogrammetry, Remote Sensing and Spatial Information Sciences, IV-2/W5: 357-364
- ❑ Hebel M, Stilla U (2012) Simultaneous calibration of ALS systems and alignment of multiview LiDAR scans of urban areas. IEEE Transactions on Geoscience and Remote Sensing, 50(6): 2364-2379
- ❑ Hebel M, Arens M, Stilla U (2013) Change detection in urban areas by object-based analysis and on-the-fly comparison of multi-view ALS data. ISPRS Journal of Photogrammetry and Remote Sensing 86 (2013): 52–64
- ❑ Hirt P (2020) Reconstruction and monitoring of urban trees based on dense 3D point point clouds. https://www.pf.bgu.tum.de/pub/2020/stilla_phd20_hirt_top.pdf
- ❑ Hoegner L, Stilla U (2018) Mobile thermal mapping for matching of infrared images with 3D building models and 3D point clouds. Quantitative InfraRed Thermography Journal, 1-19

References (2)

- Meyer T (2019) Änderungsdetektion durch Analyse von Bildsequenzen und BIM-konformen Innenraummodellen https://www.pf.bgu.tum.de/pub/2019/stilla_phd19_meyer_top.pdf
- Tessema LS, Jaeger R, Stilla U (2019) Extraction of an IndoorGML Model from an Occupancy Grid Map Constructed using 2D LiDAR. 39. Wissenschaftlich-Technische Jahrestagung der DGPF, 28: 97-110
- Tuttas S, Braun A, Borrmann A, Stilla U (2017) Acquisition and consecutive registration of photogrammetric point clouds for construction progress monitoring using a 4D BIM. PFG – Journal of Photogrammetry, Remote Sensing and Geoinformation Science, 85(1): 3-15
- Villamil Lopez C, Stilla U (2019) Using coherent scatterers in this series of high resolution SAR images for the monitoring of construction activity. ISPRS Annals of the Photogrammetry, Remote Sensing and Spatial Information Sciences, IV-2/W7: 183–187
- Xu Y, Ye Z, Huang R, Hoegner L, Stilla U (2020) Robust segmentation and localization of structural planes from photogrammetric point clouds in construction sites. Automation in Construction, 117: 103206
- Xu Y, Ye Z, Yao W, Huang R, Tong X, Hoegner L, Stilla U (2020) Classification of LiDAR point clouds using supervoxel-based detrended feature and perception-weighted graphical model. IEEE Journal of Selected Topics in Applied Earth Observations and Remote Sensing, 13: 72-88
- Zhu J, Gehrung J, Huang R, Borgmann B, Sun Z, Hoegner L, Hebel M, Xu Y, Stilla U (2020) TUM-MLS-2016: An annotated mobile LiDAR dataset of the TUM city campus for semantic point-cloud interpretation in urban areas. Remote Sensing, 12(11): 1875
- Zhu J, Xu Y, Hoegner L, Stilla U (2019) Direct co-registration of TIR images and MLS point clouds by corresponding keypoints. ISPRS Annals of the Photogrammetry, Remote Sensing and Spatial Information Sciences, IV-2/W7: 235–242